Two Copper(II) Complexes Built from a Novel Redox-Active Bipyridinium Dimer Ligand and Oxalate Anions: Synthesis, Crystal Structure and Magnetic Properties

Yan-Qiong Sun,[a] Jie Zhang,*[a] Jing-Lin Chen,[a] and Guo-Yu Yang[a]

Keywords: Copper(II) / Bipyridium dimer / Oxalate / X-ray diffraction

The synthesis of a novel V-shaped redox-active bipyridinium dimer ligand, 2,6-bis(4′-pyridyl-1′-pyridiniumyl)pyrazine (**Bpypr**) dichloride and its copper complexes, (H_2**Bpypr**)$[Cu_2(C_2O_4)_4]$ (**1**) and {[(**Bpypr**)$Cu_2(C_2O_4)_3$-$(H_2O)_2]\cdot 5H_2O\}_n$ (**2**), are described. Single-crystal X-ray diffraction studies confirm that complex **1** contains one V-shaped H_2**Bpypr** cation and two essentially planar $[Cu(C_2O_4)_2]^{2-}$ anions, which participate in two hydrogen bonds through the two N–H moieties. Complex **2** has a 1D zigzag chain structure composed of $[Cu_2(C_2O_4)_3]^{2-}$ units bridged by V-shaped **Bpypr** cations. The magnetic study revealed the occurrence of a weak ferromagnetic interaction within the dinuclear copper unit of complex **2**.

Introduction

In recent years, the design and synthesis of metal-organic coordination polymers has attracted considerable attention in supramolecular chemistry and crystal engineering,[1−5] because these supramolecular assemblies have interesting structures as well as potentially useful properties such as magnetic, catalytic, and nonlinear optical activities or electrical conductivity, amongst others.[6−9] A developing strategy in this field is to build supramolecular arrays by use of polynuclear coordination complexes as the secondary architectural units, which introduces the appealing possibility of constructing porous materials[10,11] and molecular-scale wires.[12,13] In order to produce defined architectures and interesting functions in a controlled fashion, careful selection of the metal ions, peripheral ligands and modular bridging ligands is required.[14] At present, most of the systems studied are composed of molecular subunits, containing metal ions coordinated to appropriate ligands, and which are linked by extended bridging spacers such as alkanes, alkynes, or polycyclic aromatic groups. The geometry and photoelectrochemical properties of the assemblies are generally controlled by the presence of a polynuclear coordination complex.[15−17] Currently, not many bridging ligands with electrochemical and photochemical properties are available. Bipyridinium dimers, as derivatives of the viologens, exhibit photoelectrochemical activity and a change of spin multiplicity upon external stimulus.[18−20] Their terminal N-donor atoms and π-conjugated system can provide various coordination modes and structural motifs, which enable construction of versatile molecular assemblies and incorporation of optical, electronic and magnetic properties. In this paper, we report the design and synthesis of a novel V-shaped bipyridinium dimer bridging ligand (Scheme 1), 2,6-bis(4′-pyridyl-1′-pyridiniumyl)pyrazine dichloride (**Bpypr**Cl_2), which exhibits two-step electrochemical reduction processes and photochemical activity. Two new copper complexes (H_2**Bpypr**)$[Cu_2(C_2O_4)_4]$ (**1**) and {[(**Bpypr**)$Cu_2(C_2O_4)_3(H_2O)_2]\cdot 5H_2O\}_n$ (**2**), possessing quite different architectures despite use of the same starting materials, were obtained by molecular self-assembly.

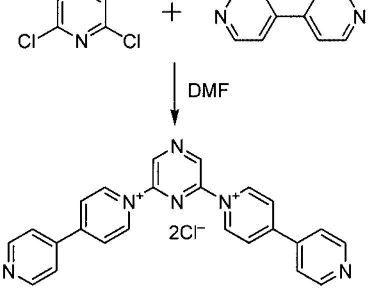

Scheme 1

---

[a] State Key Laboratory of Structural Chemistry, Fujian Institute of Research on the Structure of Matter, Chinese Academy of Sciences,
Fuzhou, Fujian 350002, China
Fax: (internat.) + 86-591-379-2871
E-mail: zhangjie@fjirsm.ac.cn

Supporting information for this article is available on the WWW under http://www.eurjic.org or from the author.

DOI: 10.1002/ejic.200400232

Results and Discussion

Redox and Photochemical Properties of the BpyprCl$_2$ Ligand

The electrochemical behavior of the **Bpypr**Cl$_2$ ligand was investigated by cyclic voltammetry in a 0.1 M acetonitrile solution of (Bu$_4$N)PF$_6$. The two-step quasi-reversible electron-transfer processes occurring at $E_{1/2} = -0.271$ V and -0.419 V vs. Ag$^+$/Ag, respectively, correspond to the first and second reduction of the **Bpypr**Cl$_2$ ligand. The photochemical activity of **Bpypr**Cl$_2$ was investigated spectrochemically in methanol solution. Under illumination with a 350-W xenon lamp, the absorption band of the ligand at 310 nm decreases in intensity and undergoes a slight blue-shift, while a new broad band appears between 400 to 600 nm, characteristic for the generation of photoinduced radicals.[21]

Structural Description

X-ray diffraction analysis reveals that complex **1** contains one V-shaped H$_2$**Bpypr** cation and two essentially planar [Cu(C$_2$O$_4$)$_2$]$^{2-}$ anions (Figure 1). Each cupric cation is coordinated by four oxygen atoms from two oxalate anions to give a square-planar geometry. The bond lengths of Cu−O range from 1.913(5) Å to 1.950(5) Å and the bond angles of O−Cu−O range from 85.3(2)° to 95.7(2)°. The H$_2$**Bpypr** ligand, with a two-fold axis passing through N(4) and N(3) atoms, is slightly twisted between the pyrazine ring and adjacent pyridyl rings, while the bipyridyl unit is close to planarity with a small dihedral angle of 7.82(25)°. Two [Cu(C$_2$O$_4$)$_2$]$^{2-}$ anions and one H$_2$**Bpypr** cation are involved in hydrogen-bonding interactions, having appropriate distances and orientation for N(1)−H(1)···O(7) [2.763(9) Å] and N(1)−H(1)···O(8) [3.012(9) Å], leading to the formation of a V-shaped dimer. These V-shaped dimers are cross-packed to yield an extended rhombic motif along the *a* axis, with [Cu(C$_2$O$_4$)$_2$]$^{2-}$ anions sitting in the center of the rhombus (Figure 2). No specific π−π stacking interactions are identifiable between N-heterocyclic rings.

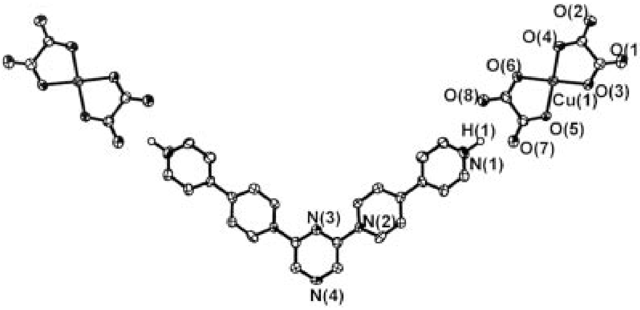

Figure 1. ORTEP drawing (50% probability level) with atom-numbering scheme of complex **1**, (H$_2$Bpypr)[Cu$_2$(C$_2$O$_4$)$_4$], showing the local coordination environment of Cu^{II}; all hydrogen atoms are omitted for clarity with the exception of H(1) on the nitrogen atom

Complex **2** possesses a one-dimensional zigzag chain structure composed of [Cu$_2$(C$_2$O$_4$)$_3$]$^{2-}$ units bridged alternately by V-shaped **Bpypr** cations. As shown in Figure 3, the crystallographically independent copper ion has an elongated octahedral geometry with the equatorial plane defined by one nitrogen atom of the **Bpypr** ligand [Cu−N: 2.026 (5) Å] and three oxalate oxygen atoms [average Cu−O: 1.961(5) Å], with the axial sites occupied by one water molecule [Cu−O 2.618(7) Å] and one oxygen atom from a centrosymmetric bridging oxalate [Cu−O 2.334(6) Å]. The bridging oxalato ligand is almost planar, with an inversion center lying in the middle of the C−C bond. The C−O bond lengths are not equivalent [1.241(8) Å, 1.283(9) Å], and those involving axial coordination are shorter. The **Bpypr** ligand, with a two-fold axis passing through N(4) and N(3) atoms, shows a nonplanar configuration. The two adjacent pyridyl rings are twisted by 16.35(52)° with respect to each other, while the dihedral angle between the pyrazine ring and the neighboring pyridyl ring is 18.61(57)°.

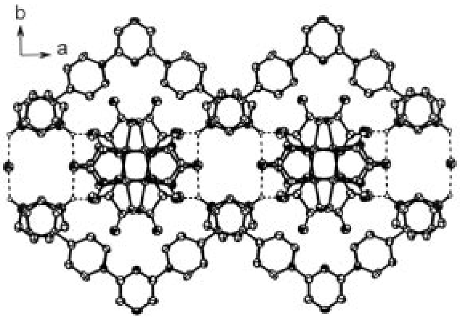

Figure 2. Packing structure for complex **1**, (H$_2$**Bpypr**)[Cu$_2$(C$_2$O$_4$)$_4$], viewed along the *c* axis; all hydrogen atoms are omitted for clarity with the exception of H(1) on the nitrogen atom

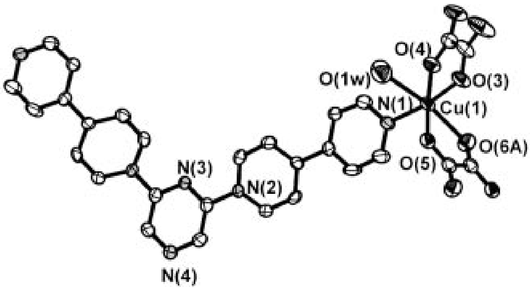

Figure 3. ORTEP drawing (50% probability level) with atom numbering scheme of complex **2**, {[(**Bpypr**)Cu$_2$(C$_2$O$_4$)$_3$(H$_2$O)$_2$]·5H$_2$O}$_n$, showing the local coordination environment of Cu^{II}; the H atoms are omitted for clarity; atom labels having "A" refer to symmetry-generated atoms

The bridging oxalate ligand coordinates to a central-symmetry-related Cu^{II} ion in bis(bidentate) fashion to give the dinuclear [Cu$_2$(C$_2$O$_4$)$_3$]$^{2-}$ ions as a secondary building unit. The Cu−Cu′ distance across the oxalate ion is 5.581(2) Å, within the range observed in dinuclear Cu^{II} complexes containing oxalate bridges in an asymmetrical bis(bidentate) coordination between the two metal centers.[22,23] V-shaped **Bpypr** cations link the [Cu$_2$(C$_2$O$_4$)$_3$]$^{2-}$ dinuclear units to form polymeric chains running along the *c* axis of the unit cell (Figure 4). These chains are stacked on top of each other along [101] to yield a subunit motif consisting of alternate rhombic sheets with a plum-blossom-like configuration. The rhombic sheets are held together further by hydrogen bonds between the terminal oxygen atoms of the uncoordinated oxalate and water molecules [O···O = 2.627(24)−3.098(27) Å], resulting in a three-dimensional supramolecular network.

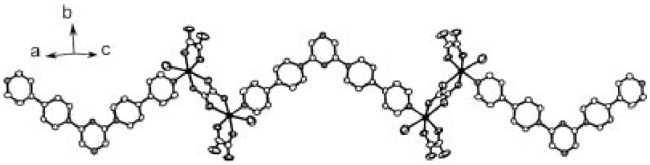

Figure 4. Zigzag chain of complex **2**, $\{[(\mathbf{Bpypr})Cu_2(C_2O_4)_3(H_2O)_2]\cdot 5H_2O\}_n$

Thermogravimetric Analysis

The thermal stabilities of the two complexes were determined by thermogravimetric analysis (TGA) under a flow of N_2. The TGA curve for **1** shows an initial weight loss of 65.23% from 40 °C to 455 °C which corresponds well to the loss of one H_2**Bpypr** cation and two oxalate anions per formula unit (calcd. 65.22%). Above 455 °C, the residual oxalate ion of complex **1** decomposes completely and the sample converts to cupric oxide above 800 °C. The TGA curve for **2** displays a three-step weight loss process. The initial weight loss of 10.31% between 50 and 120 °C corresponds to the loss of five uncoordinated water molecules per formula unit (calculated: 9.92%). The second weight loss of 50.14% is observed from 120 to 385 °C, and is attributed to the removal of two coordinated water molecules, one **Bpypr**$^{2+}$ cation and one CO molecule (from incomplete decomposition of an oxalate anion) per formula unit (calculated: 50.07%). Above 385 °C, the residual oxalate ion of complex **2** starts to decompose and the sample converts to cupric oxide at 720 °C (residual CuO, calculated: 17.53%; found 17.38%).

Electron Spin Resonance Spectroscopy

X-band powder ESR spectra of complex **1** and **2** at room temperature show broad axial signals at $g_{\parallel} = 2.1527$, $g_{\perp} = 2.0792$ ($g_{av} = 2.1163$) for **1**, and $g_{\parallel} = 2.2816$, $g_{\perp} = 2.0747$ ($g_{av} = 2.1806$) for **2**, corresponding basically to a $d_{x^2-y^2}$ ground state for the Cu^{II} ion (inverted type with $g_{\parallel} > g_{\perp} > 2.0$). The *g* values are similar to those expected for the CuO_4 chromophores of **1** with a square-planar-type geometry around the copper ion, and for those $CuNO_3O_2'$ chromophores of **2** where the copper atom is in a very elongated octahedral environment.

Magnetic Behavior

The temperature dependence of the magnetic susceptibilities was measured in the temperature range 300 to 5 K in an applied field of 10 kOe. Figure 5 shows the magnetic behavior of complex **2** in the form of the $\chi_M T$ product (χ_M is the molar magnetic susceptibility per two Cu^{II} ions) versus temperature. At room temperature, $\chi_M T$ is 0.87 $cm^3\cdot K\cdot mol^{-1}$, in agreement with the expected spin-only value for two magnetically dilute Cu^{II} centers with $S = 1/2$ ($g = 2.15$). With decreasing temperature, the $\chi_M T$ value steadily increases attaining a value of 0.99 $cm^3\cdot K\cdot mol^{-1}$ at 5 K. This behavior suggests a weak ferromagnetic interaction between the Cu^{II} ions, which is further confirmed by a positive Weiss constant ($\theta = +1.16$ K). In order to evaluate the exchange interaction between neighbouring Cu^{II} atoms, the variable-temperature susceptibility data were analyzed using Equation (1) derived[24] from the Heisenberg isotropic spin Hamiltonian ($H = -JS_1\cdot S_2$), for two coupled $S = 1/2$ ions, given by the Bleaney−Bowers expression for a dinuclear Cu^{II} compound. The interaction between adjacent dinuclear units in the 1D chain was considered in molecular-field approximation; *J* is the intradimer coupling constant between Cu^{II} ions, zJ' is the interdimer magnetic exchange, treated in the molecular field approximation. A best fit, which affords the solid line in Figure 5, was obtained with values of $g = 2.15$, $J = 3.86$ cm^{-1}, $zJ' = -0.28$ cm^{-1}. The agreement factor *R*, defined as $\Sigma[(\chi_M)_{obsd.} - (\chi_M)_{calcd.}]^2/\Sigma(\chi_M)^2_{obsd.}$, is equal to 5.73×10^{-6}. The positive *J* value demonstrates a ferromagnetic coupling between the two Cu^{II} ions.

$$\chi_M = 2Ng^2\beta^2[kT - 2zJ'/(3 + \exp(-J/kT))]^{-1}[3 + \exp(-J/kT)]^{-1} \quad (1)$$

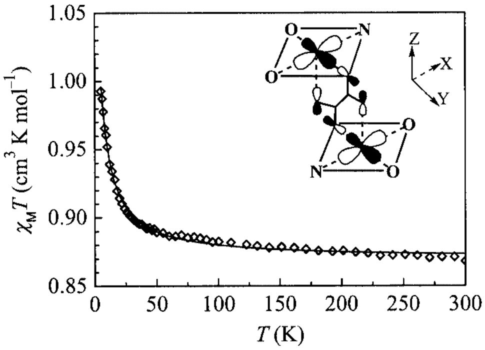

Figure 5. The temperature dependences of the product $\chi_M T$ (diamonds) for complex **2**, $\{[(\mathbf{Bpypr})Cu_2(C_2O_4)_3(H_2O)_2]\cdot 5H_2O\}_n$; the solid line corresponds to the best theoretical fit; the inset shows a model depicting the magnetic interaction in the oxalate-bridged Cu^{II} complex **2**

The complex **2** exhibits an elongated octahedral geometry, with the unpaired electron around each metal center described by a magnetic orbital of the $d_{x^2-y^2}$ type pointing toward the three oxalato oxygen atoms and one pyridyl nitrogen atom of the equatorial plane, which is perpendicular to the oxalate bridge. This situation corresponds to the coordination mode shown in the inset of Figure 5. Due to a poor overlap between the axial oxalato oxygen orbital and the metal $d_{x^2-y^2}$ orbital, a ferromagnetic coupling dominates the magnetic properties of the Cu dinuclear unit of complex **2**. The magnitude of the coupling observed is in the same range as several reported examples.[25,26]

Conclusion

A novel V-shaped redox-active bipyridinium dimer ligand, 2,6-bis(4′-pyridyl-1′-pyridiniumyl)pyrazine (**Bpypr**) dichloride has been designed and synthesized. Two new copper complexes, $(H_2\mathbf{Bpypr})[Cu_2(C_2O_4)_4]$ (**1**) and $\{[(\mathbf{Bpypr})Cu_2(C_2O_4)_3(H_2O)_2]\cdot 5H_2O\}_n$ (**2**), were obtained by assembling the **Bpypr**Cl_2 ligand with $(NH_4)_2Cu(C_2O_4)_2$. The 1-D zigzag chain of **2** is composed of $[Cu_2(C_2O_4)_3]^{2-}$ units bridged by V-shaped **Bpypr** cations in an alternating fashion. The variant assembly modes of **Bpypr** ligand with $(NH_4)_2Cu(C_2O_4)_2$ provide a great potential for construction of multifunctional organic-inorganic hybrid materials and for the observation of important structure-property relationships. More physical properties and further assemblies of the **Bpypr** ligand with other anionic donors is in progress.

Experimental Section

General Remarks: All chemicals were used as purchased without purification except those used for electrochemical measurements. The ^{1}H NMR spectrum was recorded with a Varian Unity 500 MHz spectrometer. IR spectra were measured as KBr pellets with a Bomem BM102 FT-IR in the range 400−4000 cm^{-1}. The elemental analyses were determined using a Vario EL III CHNOS elemental analyzer. Thermogravimetric data were collected with a Mettler Toledo TGA/SDTA 851^e analyzer under a stream of nitrogen at a heating rate of 5 °C/min. ESR spectra were recorded with a Bruker ER-420 spectrometer at the X-band frequency. Variable-temperature magnetic susceptibilities were measured from 300 K to 5 K with an applied field strength of 10 KOe using a Quantum Design MPMS-7 magnetometer. Diamagnetic corrections were estimated from Pascal's constants. Photochemistry of the samples in KBr pellets was investigated using a 350-W Xenon lamp. The cyclic voltammogram was obtained by use of a Perkin-Elmer potentiostat/galvanostat model 263A in 1 mM acetonitrile solution containing 0.1 M $(Bu_4N)PF_6$ as supporting electrolyte at a scan rate of 100 mV·s^{-1}. Platinum and glassy graphite were used as working and counter electrodes, respectively. Potentials were referenced to Ag/AgCl.

Preparation of the BpyprCl$_2$ Ligand: A mixture of 4,4′-bipy(3.12 g, 20 mmol) and 2,6-dichloropyrazine (1.47 g, 10 mmol) was dissolved in 8 mL of DMF. After stirring at 120 °C under nitrogen for 4 h, the solution was concentrated to a small volume under reduced pressure. Then an excess of hot benzene was added and the precipitate was collected by filtration, washed with hot benzene and dried in vacuo to afford a pale yellow powder (1.62 g, 35.3%). ^{1}H NMR ($CDCl_3$, 500MHz): δ = 8.12 (d, 4 H), 8.85 (d, 4 H), 8.89 (d, 4 H), 9.88 (d, 4 H), 9.92 (s, 2 H) ppm. IR (KBr): $\tilde{\nu}$ = 3478 (s), 3413 (s), 3118 (w), 3033 (w), 1634 (vs), 1597 (m), 1557 (m), 1463 (w), 1438 (s), 1412 (s), 1347 (w), 1281 (m), 1263 (m), 1212 (m), 1161 (w), 1019 (m), 866 (m), 821 (s), 754 (m), 718 (m), 637 (w), 619 (w), 538 (w), 501 (m) cm^{-1}.

Synthesis of $(H_2\mathbf{Bpypr})[Cu_2(C_2O_4)_4]$ (1): A mixture of **Bpypr**Cl_2 (102.2 mg, 0.2 mmol) and $CuCl_2$ (34 mg, 0.2 mmol) was dissolved in water. The resulting solution was layered with an H_2O/DMSO (5:1, v/v) solution (20 mL) of $(NH_4)_2Cu(C_2O_4)_2$ (55.1 mg, 0.2 mmol) in a 1:1 ratio in a straight glass tube. Black-green prism crystals were obtained by slow interface diffusion after a few days. Yield 11%. IR (KBr): $\tilde{\nu}$ = 3556 (m), 3454 (m), 3114 (w), 3037 (w), 1707 (w), 1652 (vs), 1431 (s), 1415 (m), 1378 (s), 1278 (m), 1241 (m), 1201 (m), 1007 (m), 818 (m), 792 (m), 551 (w), 497 (m) cm^{-1}. $C_{32}H_{20}Cu_2N_6O_{16}$ (871.62): calcd. C 44.10, H 2.31, N 9.64; found C 43.76, H 1.86, N 9.54.

Synthesis of $\{[(\mathbf{Bpypr})Cu_2(C_2O_4)_3(H_2O)_2]\cdot 5H_2O\}_n$ (2): A mixture of **Bpypr**Cl_2 (102.2 mg, 0.2 mmol) and $CuCl_2$ (34 mg, 0.2 mmol) was dissolved in water. The resulting solution was layered with an H_2O/DMSO (5:1, v/v) solution (20 mL) of $(NH_4)_2Cu(C_2O_4)_2$ (55.1 mg, 0.2 mmol) in a 1:1 ratio in a straight glass tube. Green needle crystals were obtained by slow interface diffusion after a few days. Yield 32%. IR (KBr): $\tilde{\nu}$ = 3416 (s), 3121 (w), 3038 (w), 1691 (vs),

Table 1. Crystallographic data for complexes **1** and **2**

	1	**2**
Empirical formula	$C_{32}H_{20}Cu_2N_6O_{16}$	$C_{30}H_{32}Cu_2N_6O_{19}$
Formula mass	871.62	907.70
Crystal system	monoclinic	monoclinic
Space group	*C*2/*c*	*C*2/*c*
T [K]	293	293
a [Å]	12.5637(5)	15.6288(6)
b [Å]	18.3206(8)	19.8960(1)
c [Å]	12.9832(3)	12.7179(5)
β [°]	116.49(1)	90.436(2)
V [Å^3]	2988.32(19)	3507.97(19)
Z	4	4
$D_{calcd.}$ [g·cm^{-3}]	1.937	1.719
μ [mm^{-1}]	1.523	1.307
F(000)	1760	1856
Goodness-of-fit on F^2	1.069	1.099
Reflections collected/unique	4329/2466 [*R*(int) = 0.0505]	5279 / 3031 [*R*(int) = 0.0446]
Data/restraints/parameters	2466/0/258	3031 / 0 / 272
R_1/wR_2 [$I > 2\sigma(I)$]	0.0730/0.1453	0.0649/0.1597
R_1/wR_2 (all data)	0.1088/0.1660	0.1183/0.2091
Largest difference peak and hole	0.671 and −0.608 e·Å^{-3}	0.566 and −0.454 e·Å^{-3}

$R1 = \Sigma||F_o| - |F_c||/\Sigma|F_o|$. $wR2 = \{\Sigma[w(F_o^2 - F_c^2)^2]/\Sigma[w(Fo^2)^2]\}^{1/2}$ where $w = 1/[\sigma^2(F_o^2) + (AP)^2 + BP]$, with A = 0.0444 (**1**) and 0.1077 (**2**), B = 41.3993 (**1**) and 9.3117 (**2**), $P = (F_o^2 + 2F_c^2)/3$.

Table 2. Selected bond lengths [Å] and angles [°] for **1** and **2**

Complex **1**			
Cu(1)−O(4)	1.913(5)	Cu(1)−O(5)	1.936(5)
Cu(1)−O(3)	1.934(5)	Cu(1)−O(6)	1.950(5)
O(4)−Cu(1)−O(3)	85.6(2)	O(3)−Cu(1)−O(5)	95.7(2)
O(4)−Cu(1)−O(6)	93.3(2)	O(5)−Cu(1)−O(6)	85.3(2)
O(4)−Cu(1)−O(5)	177.4(2)	O(3)−Cu(1)−O(6)	178.8(2)
Complex **2**			
Cu(1)−O(4)	1.959(5)	Cu(1)−N(1)	2.026(5)
Cu(1)−O(3)	1.958(5)	Cu(1)−O(6)#1	2.334(6)
Cu(1)−O(5)	1.965(5)	Cu(1)−O1W	2.618(7)
O(4)−Cu(1)−O(3)	83.6(2)	O(5)−Cu(1)−O(6)#1	77.11(19)
O(3)−Cu(1)−O(5)	89.4(2)	N(1)−Cu(1)−O(6)#1	94.7(2)
O(4)−Cu(1)−N(1)	94.5(2)	O(4)−Cu(1)−O(6)#1	103.1(2)
O(5)−Cu(1)−N(1)	86.7(2)	O(3)−Cu(1)−O(6)#1	94.8(2)

Symmetry transformations used to generate equivalent atoms: #1: $-x + 1/2, -y + 1/2, -z + 1$.

1636 (s), 1432 (s), 1413 (s), 1298 (m), 1289 (m), 1208 (m), 1011 (m), 822 (m), 798 (m), 717 (w), 555 (w), 499 (m) cm^{-1}. $C_{30}H_{32}Cu_2N_6O_{19}$ (907.70): calcd. C 39.70, H 3.55, N 9.26; found C 39.25, H 3.27, N 9.09.

X-ray Crystallography: Data sets for **1** and **2** were collected at room temperature using a Siemens SMART CCD diffractometer with graphite-monochromated Mo-K_α (λ = 0.71073 Å) radiation in the ω- and φ-scanning mode. An empirical absorption correction was applied using the SADABS program. The structures were solved by direct methods and refined by full-matrix least-squares on F^2 using the SHELXTL-97 program package.[27] All hydrogen atoms were generated geometrically (C−H = 0.93 Å) with the exception of the hydrogen atoms of all free water molecules and H(1) of **1**. H(1) of **1** was located in the difference Fourier map and its position and isotropic displacement parameters were refined. The crystallographic data for complexes **1** and **2** are listed in Table 1. Selected bond lengths and angles are shown in Table 2. CCDC-220468 (**1**) and -220467 (**2**) contain the supplementary crystallographic data for this paper. These data can be obtained free of charge at www.ccdc.cam.ac.uk/conts/retrieving.html [or from the Cambridge Crystallographic Data Centre, 12 Union Road, Cambridge CB2 1EZ, UK; Fax: (internat.) + 44-1223-336-033; E-mail: deposit@ccdc.cam.ac.uk].

Acknowledgments

The authors thank the National Natural Science Foundation of China (No. 20201010/50372069), the Ministry of Personnel of China, and the Natural Science Foundation of Fujian Province for financial support. The authors are also grateful to Prof. Zhong-Ning Chen for electrochemical measurements.

---

[1] H. J. Choi, M. P. Suh, *J. Am. Chem. Soc.* **1998**, *120*, 10622−10628.

[2] A. K. Cheetham, G. Férey, T. Loiseau, *Angew. Chem. Int. Ed.* **1999**, *38*, 3268−3292.

[3] D.-L. Long, A. J. Blake, N. R. Champness, M. Schröder, *Chem. Commun.* **2000**, 1369−1370.

[4] C. Janiak, *Dalton Trans.* **2003**, 2781−2804.

[5] S. L. James, *Chem. Soc. Rev.* **2003**, *32*, 276−288.

[6] E. Coronado, J. R. Galán-Mascarós, C. J. Gómez-García, V. Laukhin, *Nature* **2000**, *408*, 447−449.

[7] S. Karasawa, Y. Sano, T. Akita, N. Koga, T. Itoh, H. Iwamura, P. Rabu, M. Drillon, *J. Am. Chem. Soc.* **1998**, *120*, 10080−10087.

[8] O. M. Yaghi, H. Li, C. Davis, D. Richardson, T. L. Groy, *Acc. Chem. Res.* **1998**, *31*, 474−484.

[9] P. G. Lacroix, I. Malfant, S. Benard, P. Yu, E. Riviere, K. Nakatani, *Chem. Mater.* **2001**, *13*, 441−449.

[10] M. Eddaoudi, D. B. Moler, H. L. Li, T. M. Reineke, M. O'Keeffe, O. M. Yaghi, *Acc. Chem. Res.* **2001**, *34*, 319−330.

[11] H. K. Chae, J. Kim, O. D. Friedrichs, M. O'Keefe, O. M. Yaghi, *Angew. Chem. Int. Ed.* **2003**, *42*, 3907−3909.

[12] R. L. Carroll, C. B. Gorman, *Angew. Chem. Int. Ed.* **2002**, *41*, 4378−4400.

[13] J. L. Chen, L. Y. Zhang, Z. N. Chen, L. B. Gao, M. Abe, Y. Sasaki, *Inorg. Chem.* **2004**, *43*, 1481−1490.

[14] L. De Cola, P. Belser, *Coor. Chem. Rev.* **1998**, *177*, 301−346.

[15] C. H. Londergan, J. C. Salsman, S. Ronco, L. M. Dolkas, C. P. Kubiak, *J. Am. Chem. Soc.* **2002**, *124*, 6236−6237.

[16] Y. Hoshino, S. Higuchi, J. Fiedler, C.-Y. Su, A. Knodler, B. Schwederski, B. Sarkar, H. Hartmann, W. Kaim, *Angew. Chem. Int. Ed.* **2003**, *42*, 674−677.

[17] F. A. Cotton, J. P. Donahue, C. A. Murillo, *J. Am. Chem. Soc.* **2003**, *125*, 5436−5450.

[18] P. Rajakumar, K. Srinivasan, *Eur. J. Org. Chem.* **2003**, 1277−1284.

[19] T. Iyoda, M. M. Matsushita, T. Kawai, *Pure Appl. Chem.* **1999**, *71*, 2079−2084.

[20] J. Zhang, M. M. Matsushita, X. X. Kong, J. Abe, T. Iyoda, *J. Am. Chem. Soc.* **2001**, *123*, 12105−12106.

[21] M. M. Matsushita, M. Morikawa, T. Kawai, T. Iyoda, *Mol. Cryst. and Liq. Cryst.* **2000**, *343*, 87−96.

[22] M. Julve, M. Verdaguer, A. Gleizes, M. Philoche-Levisalles, O. Kahn, *Inorg. Chem.* **1984**, *23*, 3808−3818.

[23] Z. Smekal, Z. Travnicek, F. Loret, J. Marek, *Polyhedron* **1999**, *18*, 2787−2793.

[24] O. Kahn, *Molecular Magnetism*, VCH Publishers, New York, **1993**, p. 132.

[25] O. Costisor, M. Brezeanu, Y. Journaux, K. Mereiter, P. Weinberger, W. Linert, *Eur. J. Inorg. Chem.* **2001**, 2061−2066.

[26] Z. Smékal, Z. Trávníček, F. Lloret, J. Marek, *Polyhedron* **1999**, *18*, 2787−2793.

[27] G. M. Sheldrick, *SHELXL-97, Program for the Refinement of Crystal Structures*, University of Göttingen, Göttingen, Germany, **1997**.

Received March 23, 2004
Early View Article
Published Online August 3, 2004